American Mineralogist, Volume 68, pages 95–105, 1983

Diffusion data for clinopyroxenes from homogenization and self-diffusion experiments

JOHN B. BRADY

Department of Geology
Smith College
Northampton, Massachusetts 01063

AND ROBERT H. MCCALLISTER[1]
Department of Geosciences
Purdue University
West Lafayette, Indiana 47907

Abstract

Kinetic experiments involving the homogenization of fine-scale, coherent (001) pigeonite lamellae in a sub-calcic diopside have been used to constrain Ca–Mg interdiffusion coefficients for clinopyroxenes. At 1150°–1250°C and 25 kbar, "average" Ca–Mg effective binary interdiffusion coefficients are described by

$$\tilde{D} = (3.89 \times 10^{-7}) \exp(-360.87 \text{ kJ}/RT) \quad (\text{m}^2/\text{sec})$$

$$(\tilde{D} = (3.89 \times 10^{-3}) \exp(-86.25 \text{ kcal}/RT) \quad (\text{cm}^2/\text{sec}))$$

with an uncertainty of a factor of 2. Because of the large thermodynamic effect on diffusion near a solvus, actual interdiffusion coefficients should vary by an order of magnitude or more with composition for the conditions of these experiments. Attempts to obtain Ca and Fe self-diffusion coefficients in natural diopsides at 1 atm using ^{45}Ca and ^{57}Fe tracers and thin-film, autoradiographic techniques were unsuccessful. These negative results place upper bounds on the Ca and Fe self-diffusion coefficients in diopside that are consistent with the results of the homogenization experiments.

Introduction

Comparatively few data are available on diffusion in pyroxenes. Although several measurements of tracer diffusion or self-diffusion have been reported (Sneeringer and Hart, 1978; McCallister and Brady, 1979), we know of no published measurements of chemical diffusion coefficients. Negative results reported by Huebner *et al.* (1975, p. 543) suggested that it might be difficult to produce the good interface required for a chemical exchange between two pyroxene crystals. Therefore, we considered studying exsolved natural pyroxenes with presumably well-annealed or even coherent interfaces between chemically distinct exsolution lamellae. Previous work by one of us (McCallister, 1977) indicated that homogenization of finely exsolved clinopyroxenes (lamellar wavelength λ = 15–30 nm) was comparatively rapid at high pressures. We have studied the rate of this homogenization for a natural pyroxene and interpret our results below on the assumption that the homogenization rate is diffusion-limited. Brady and Yund (1983) have shown that diffusion coefficients obtained from similar homogenization experiments with alkali feldspars agree well with diffusion coefficients obtained by other methods. Because of the small size of the exsolution lamellae, very small diffusion coefficients are accessible through kinetic studies of this kind.

Experimental procedures

A subcalcic diopside megacryst from the Mabuki kimberlite, Tanzania, containing coherent pigeonite exsolution lamellae parallel to (001) was used for most experiments. The wavelength λ for these lamellae is 19.8±1.5 nm as determined from examination of a thin foil using a JEOL 200CX transmission electron microscope. Comparable results were ob-

[1]Present address: Exxon Production Research Co., Reservoir Evaluation, P.O. Box 2189, Houston, Texas 77001.

0003–004X/83/0102–0095$02.00

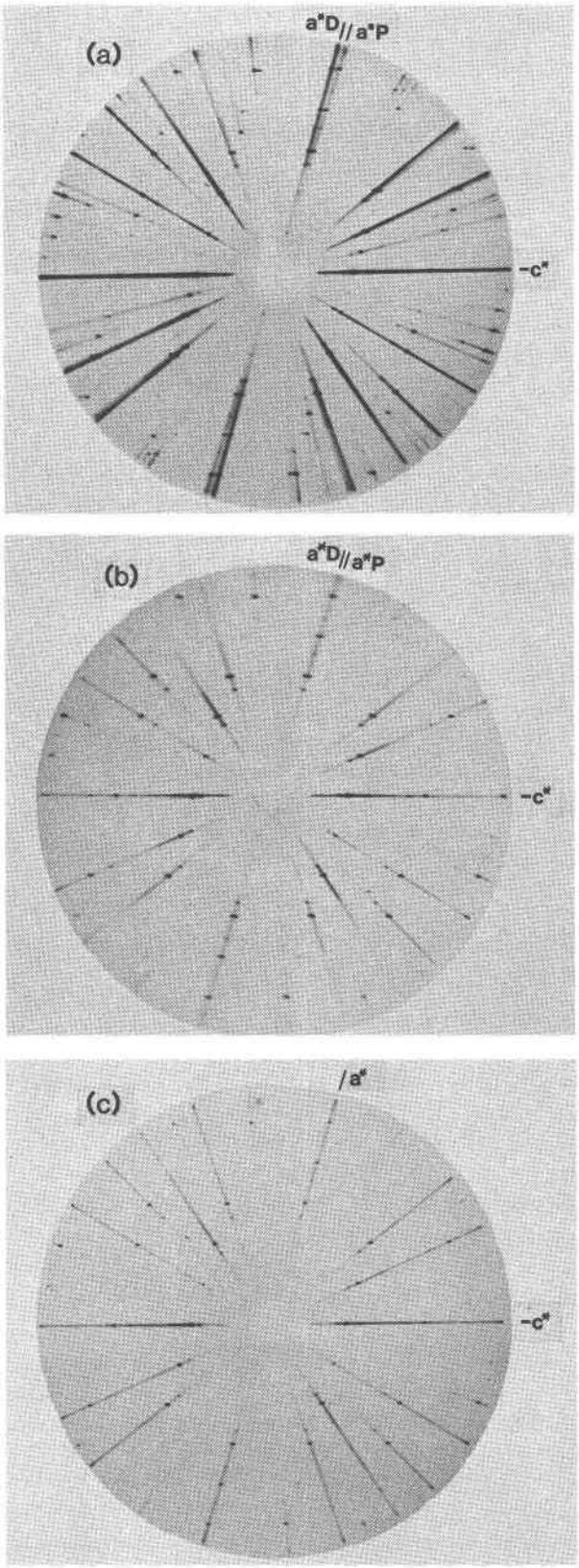

tained using a pyroxene from the Thaba Putsoa kimberlite, Lesotho (Nixon and Boyd, 1973, PHN-1611). The Mabuki pyroxene has a very uniform bulk composition represented by the formula (based on four cations) $K_{0.001}Na_{0.094}Ca_{0.525}Mg_{1.104}Fe^{+2}_{0.174}Mn_{0.003}Ni_{0.002}Cr_{0.008}Al_{0.107}Ti_{0.010}Si_{1.968}O_{5.990}$ determined by electron microprobe. The coherency on (001) of the diopside host, space group $C2/c$, and pigeonite lamellae, space group $P2_1/c$, is demonstrated by a common c^* axis and identical a and b unit cell dimensions for both pyroxenes as observed on precession X-ray photographs. Initially, β = 106°40′ for the diopside and 108°39′ for the pigeonite. Compositions of the diopside host and pigeonite lamellae can be estimated from the measured β's using the data of Turnock *et al.* (1973) and by assuming that both phases have the same ratio (0.136) of Fe to (Fe+Mg). All pyroxene compositions reported below are calculated in this manner. The ratios of Ca to (Ca+Mg+Fe) so calculated, 0.348 for the diopside and 0.077 for the pigeonite, were not corrected for coherency strain (see Tullis and Yund, 1979).

Crystals of the Mabuki pyroxene were packed in a Pt capsule using powdered carbon as a filler. The capsule was then sealed and annealed for periods from 10 minutes to 4 days in a ½ inch piston cylinder apparatus. Most runs were made at 25 kbar (no friction correction) and at temperatures from 1050° to 1250°C as measured by Pt/Pt10%Rh thermocouples. Following each run, a single crystal was mounted and oriented for a b-axis precession X-ray photograph. Progress of the homogenization was marked by the separation of the β's of the diopside and pigeonite on the precession photos (Fig. 1).

Results

The results of our experiments are summarized in Table 1. Estimated lamellar compositions and "average" diffusion coefficients (see below) are listed along with the measured values of temperature, time, β (diopside), and β (pigeonite). Compositions were calculated from the Turnock *et al.* (1973) data as discussed above and should be considered as approximations to compare with the models presented below.

Although all runs were in the stability field of orthopyroxene + diopside (Lindsley *et al.*, 1981),

Fig. 1. b-axis precession X-ray photographs of the Mabuki pyroxene (a) prior to any experiments, (b) after 15 minutes at 1150°C, and (c) after 25 minutes at 1250°C (all at 25 kbar).

Table 1. Homogenization data

	Run	T(°C)	t(sec)	β(Pig)	β(Di)	X(Pig)	X(Di)	$\tilde{D}$(cm^2/sec)
	PX107	1050	$7.2 \times 10^{+3}$	108°18'	106°28'	0.27	0.74	
	PX106	1050	$2.88 \times 10^{+4}$	108°15'	106°25'	0.29	0.76	
	PX120	1050	$2.88 \times 10^{+4}$	108°10'	106°26'	0.32	0.75	
+	PX109	1100	$3.6 \times 10^{+3}$	108°15'	106°40'	0.29	0.70	$<1.4 \times 10^{-16}$
+	PX121	1100	$7.2 \times 10^{+3}$	108°03'	106°43'	0.36	0.68	$<6.9 \times 10^{-17}$
+	PX124	1100	$9.0 \times 10^{+3}$	108°11'	106°41'	0.32	0.69	$<5.6 \times 10^{-17}$
+	PX110	1100	$2.52 \times 10^{+4}$	108°07'	106°42'	0.34	0.69	$<2.0 \times 10^{-17}$
+	PX111	1100	$8.79 \times 10^{+4}$	108°00'	106°50'	0.37	0.66	$>5.7 \times 10^{-18}$
++	PX114	1100	$3.46 \times 10^{+5}$	108°10'	107°00'	0.32	0.62	
*	PX119	1100	$3.46 \times 10^{+5}$	108°04'	106°42'	0.36	0.69	
	PX104	1150	$9.0 \times 10^{+2}$	107°53'	106°58'	0.41	0.63	$<5.6 \times 10^{-16}$
**	PX101	1150	$1.8 \times 10^{+3}$	107°12'	107°12'	0.56	0.57	$<2.8 \times 10^{-16}$
	PX118	1150	$3.0 \times 10^{+3}$	-------	107°16'	----	0.56	$>1.7 \times 10^{-16}$
	PX102	1150	$7.2 \times 10^{+3}$	-------	107°15'	----	0.56	$>6.9 \times 10^{-17}$
	PX103	1150	$2.88 \times 10^{+4}$	-------	107°15'	----	0.56	
	PX112	1200	$6.0 \times 10^{+2}$	107°40'	107°10'	0.46	0.58	$<8.3 \times 10^{-16}$
	PX115	1200	$1.2 \times 10^{+3}$	-------	107°15'	----	0.56	$>4.2 \times 10^{-16}$
	PX105	1250	$9.0 \times 10^{+2}$	-------	107°13'	----	0.57	$>5.6 \times 10^{-16}$

\+ Kinetics affected by movement of coherent interface.
++ No longer coherent.
* Homogenized at 1150°C for 2 hours then annealed at 1100°C. Exsolution apparently occurred, but lamellae were not coherent after 4 hours at 1100°C.
** Pigeonite reflections still faintly visible on precession photo.

no orthopyroxene was observed in any of the runs. At 1250°, 1200°, and 1150°C homogenization was complete in 50 minutes or less. At 1100° and 1050°C, complete homogenization did not occur, even for runs of four days duration. We interpret these data as indicating the presence of a metastable coherent solvus for iron-poor clinopyroxenes at 25 kbar (compare Ross *et al.*, 1973). The data are shown in Figure 2 with the inferred solvus projected onto the enstatite–diopside–temperature plane. Half-filled data points represent final diopside or pigeonite lamellar compositions (see caption). Solid data points are final homogenized pyroxene compositions. In each case the starting compositions were the same: pigeonite = 15.4 mole percent Di ($CaMgSi_2O_6$), 84.6 mole percent En ($Mg_2Si_2O_6$); diopside = 69.6% Di, 30.4% En. All of the composition changes were toward the solvus from the outside, except for the diopside compositions at 1050°C, which became richer in Di. The solvus shown was fit to the observed "final" diopside and pigeonite compositions using the method of Thompson and Waldbaum (1969a, p.681). The single open data point represents the bulk composition of a sample (PX119) that was homogenized at 1150°C for two hours, then annealed at 1100°C for four days. Because exsolution was observed in this sample, we concluded that the point was inside the solvus. Evidence for noncoherency was observed in the precession photos of PX119 and PX114, both four day runs. The position of the solvus has not been reversibly defined, but all evidence is consistent with a coherent solvus located roughly as shown in Figure 2.

Diffusion

The homogenization process requires diffusion in only one dimension, due to the regular geometry of the exsolution lamellae. Because each of the lamellae is bisected by a plane of symmetry, only one host-lamella pair need be considered. For the special case of binary diffusion with a single constant interdiffusion coefficient, a solution to the diffusion equation for the lamellar geometry is given by Crank (1975, p.63) in the form of an infinite series. This solution is shown graphically in Figures 3a and 3b for the host-lamellar width ratio of the Mabuki pyroxenes. The normalized concentration profile is shown in Figure 3a at various stages of the homogenization. The concentration difference between the centers of adjacent lamellae is shown in Figure 3b as a function of a dimensionless variable ($\tilde{D}t/L^2$)

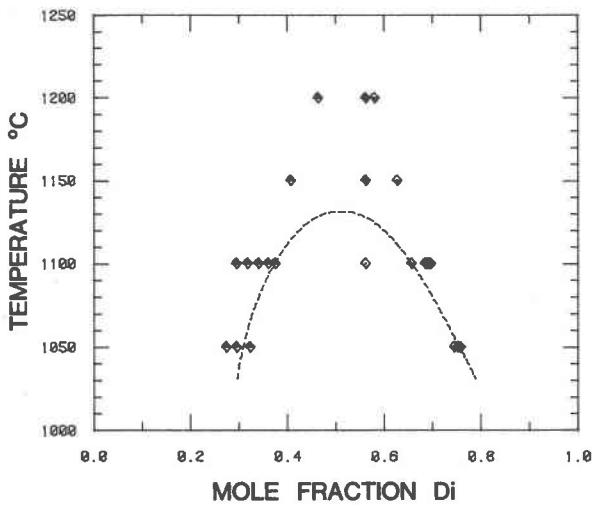

Fig. 2. Estimated compositions of diopside (◆) and pigeonite (◆) lamellae following homogenization experiments. Fully homogenized compositions (◆) are shown at 1150° and 1200°C. One sample homogenized at 1150° was exsolved by heating at 1100°C (◇). The dashed line is our estimate of the position of a metastable coherent solvus for the clinopyroxenes at 25 kbar. Compositions have been projected onto the enstatite ($Mg_2Si_2O_6$)–diopside ($CaMgSi_2O_6$) composition axis as described in the text.

that marks the progress of the homogenization. $\tilde{D}$ is the interdiffusion coefficient (cm^2/sec), t is time (sec), and L is the distance (cm) between the centers of adjacent lamellae ($\lambda/2$). Because β of a clinopyroxene is a function of composition, the difference in β between the diopside host and pigeonite guest in our experiments should decay in a manner similar to that shown in Figure 3b.

Although it is possible to trace in detail the progress of the homogenization in terms of the difference in β between the two pyroxenes, it is not warranted in this case due to the complications discussed below. The data are most appropriately used to determine either complete or incomplete homogenization. We conclude from Figure 3b that if no difference in β between the diopside and pigeonite is measureable (*i.e.*, only one diffraction pattern visible), the dimensionless parameter ($\tilde{D}t/L^2$) would be greater than 0.5, if the diffusion coefficient were independent of composition. Similarly, if two diffraction patterns and two values of β are visible on the precession photo, ($\tilde{D}t/L^2$) would be less than 0.5. Because the duration of each experiment (t) and the lamellar spacing (L = 10 nm) are known, upper and lower bounds to an "average" $\tilde{D}$ may be calculated. "Average" $\tilde{D}$'s calculated in this manner are listed in Table 1.

Unfortunately, neither the assumption of binary Ca–Mg exchange nor the assumption of a constant interdiffusion coefficient can be correct. The presence of chemical components other than En and Di in the Mabuki pyroxene means that multicomponent diffusion probably occurred. However, the one-dimensional geometry of the sample and its Ca–Mg-rich composition satisfy the requirements for the successful use of an "effective binary (Ca–Mg)

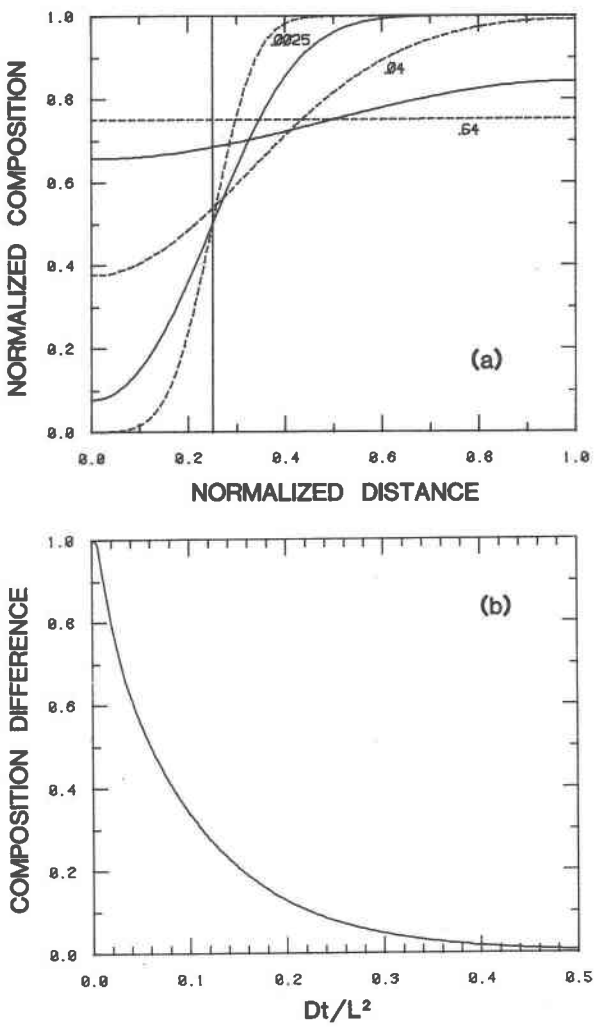

Fig. 3. (a) Composition profiles for stages in the ideal homogenization of two exsolution lamellae are shown in terms of dimensionless composition and distance variables, assuming a single constant interdiffusion coefficient. The initial width ratio of the two lamellae is 1:3. The profiles shown are for values of the dimensionless time variable $\tilde{D}t/L^2$ (see text) of 0, 0.0025, 0.01, 0.04, 0.16, and 0.64. (b) The normalized difference in composition between the centers of the two lamellae during the homogenization described in (a) is shown as a function of the dimensionless time parameter $\tilde{D}t/L^2$. Homogenization is essentially complete when $\tilde{D}t/L^2 > 0.5$.

diffusion coefficient'' (Cooper, 1968). Thus, neglecting the presence and movement of other chemical species should not seriously reduce the usefulness of our results.

Because the experiments were conducted for compositions, temperatures, and pressures near a solvus (see below), the interdiffusion coefficient may vary by two orders of magnitude or more over the composition range considered. Near a solvus there is a thermodynamic ''drag'' that inhibits normal ''random walk'' diffusion. Within a spinodal this ''thermodynamic effect'' can lead to exsolution processes involving diffusion up concentration gradients. The magnitude of the thermodynamic effect for binary interdiffusion is given by the expression:

$$\frac{\mathrm{d}\ \ln\ a(\mathrm{i})}{\mathrm{d}\ \ln\ X(\mathrm{i})} \tag{1}$$

where a(i) is the molar thermodynamic activity and X(i) the mole fraction of either of the two components i (see Darken, 1948; Brady, 1975).

To see the nature of the thermodynamic effect, consider the relation between the self-diffusion coefficients of Ca and Mg and the binary Ca–Mg interdiffusion coefficient in an iron-free diopside–clinoenstatite solid solution. The desired relation, which may be obtained from charge-balance and thermodynamic arguments (Manning, 1968; Brady, 1975), is

$$\tilde{D}(\mathrm{Ca\text{–}Mg}) = \left(\frac{D^*(\mathrm{Mg})D^*(\mathrm{Ca})}{X(\mathrm{En})D^*(\mathrm{Mg}) + X(\mathrm{Di})D^*(\mathrm{Ca})}\right)\left(\frac{\mathrm{d}\ \ln\ a(\mathrm{Di})}{\mathrm{d}\ \ln\ X(\mathrm{Di})}\right) \tag{2}$$

where $\tilde{D}$(Ca–Mg) is the Ca–Mg interdiffusion coefficient, D*(Mg) and D*(Ca) are the Mg and Ca self-diffusion coefficients, a(Di) is the molar activity of diopside, and X(Di) is the mole fraction of diopside in a $(CaMgSi_2O_6)$–$(Mg_2Si_2O_6)$ pyroxene. This expression may be fully evaluated only for systems where both tracer diffusion coefficients and thermodynamic data are available (*e.g.*, Reynolds *et al.*, 1957; Brady and Yund, 1983). Because self-diffusion coefficients are not available for clinopyroxenes (see below), the variation of the interdiffusion coefficient with composition must be evaluated on the basis of thermodynamic data alone.

Although the thermodynamic properties of iron-free clinopyroxenes are fairly well known (see Lindsley *et al.*, 1981), the Mabuki pyroxene should obey a somewhat different equation of state. Stresses from the coherency of the lamellae (Tullis and Yund, 1979) require that a coherency-corrected molar Gibbs function for clinopyroxenes be used to determine the thermodynamic factor (1). We have used the solvus shown in Figure 2 along with the method of Thompson and Waldbaum (1969b, p. 836) to obtain the following Margules parameters (WG) for the apparent excess molar Gibbs function for our pseudo-binary pyroxenes:

$$\begin{aligned} WG(\mathrm{En}) &= 46910.76 - 16.719T\ (\mathrm{J/mole}) \\ WG(\mathrm{Di}) &= 6741.85 + 11.799\ T\ (\mathrm{J/mole}) \end{aligned} \tag{3}$$

where T is the temperature in degrees K. These parameters are poorly constrained by the data shown in Figure 2 and should be considered only rough approximations. It can be shown that the thermodynamic factor (1) is equivalent to the expression

$$1 + \left(\frac{X(\mathrm{En})X(\mathrm{Di})}{RT}\right) \times \left(\begin{array}{l} WG(\mathrm{En})\ [2X(\mathrm{En}) - 4X(\mathrm{Di})] \\ \quad + WG(\mathrm{Di})\ [2X(\mathrm{Di}) - 4X(\mathrm{En})] \end{array}\right) \tag{4}$$

The thermodynamic factor obtained from equations (3) and (4) is shown as the solid curves in Figures 4a and 4b for temperatures of 1150° and 1250°C. The dashed lines in Figures 4a and 4b show the ''temperature adjusted'' thermodynamic factor calculated from the excess Gibbs function given by Lindsley *et al.* (1981, p. 168) for iron-free clinopyroxenes at 25 kbar. The Lindsley *et al.* data shown are for temperatures in the same position relative to their critical temperature (1500°C) as the listed temperatures are relative to the critical temperature (1132°C) shown in Figure 2. The fact that the two curves agree fairly well for all temperatures suggests that the exact shape of the solvus is not required for estimating the thermodynamic effect.

The important features of Figure 4 are the magnitude and variation of the thermodynamic factor. Clearly the interdiffusion coefficient in our homogenization experiments could not have been constant and may have varied by up to two orders of magnitude with composition. This would be true even if the Ca and Mg self-diffusion coefficients were identical, which is unlikely. To examine the consequences of a non-constant diffusion coefficient on the homogenization process, a finite-difference computer model was developed. Homogeniza-

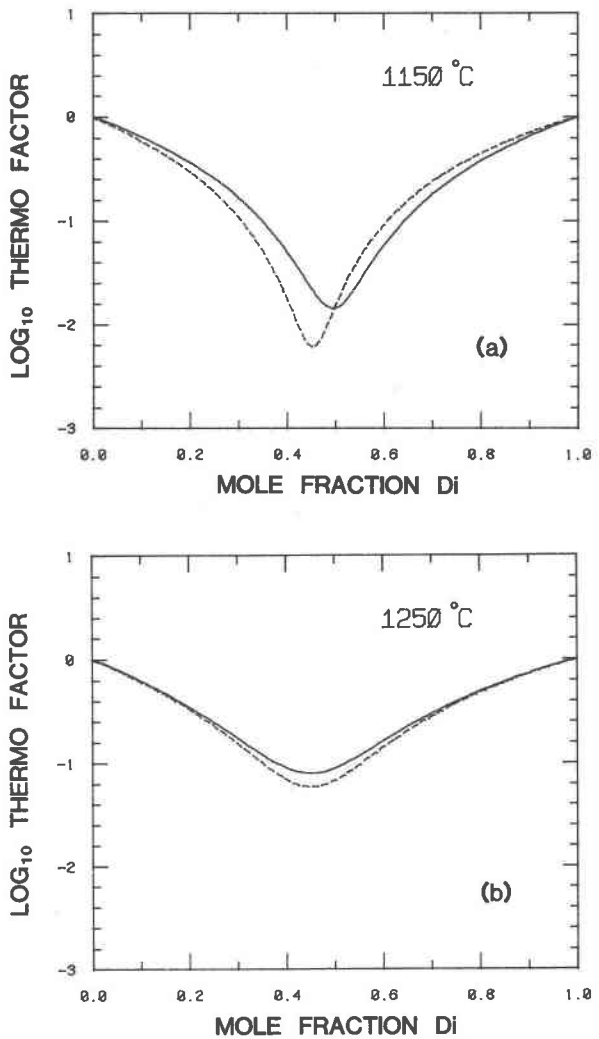

Fig. 4. The dimensionless thermodynamic factor of equation (1) is shown here as a function of pyroxene composition (En-Di) at 25 kbar and (a) 1150°C and (b) 1250°C. The solid curves are calculated from equations (3). The dashed curves are calculated from the data of Lindsley *et al.* (1981) as described in the text.

tion was simulated using a composition-dependent diffusion coefficient calculated from (2) using a thermodynamic factor calculated from (3) and (4) and assuming that the self-diffusion coefficients D*(Ca) and D*(Mg) are identical and independent of composition. The results of the simulation for 1150°, 1200°, and 1250°C are shown in Figure 5, analogous to Figure 3b. Figure 5 shows the normalized difference between the compositions of the centers of the lamellae as a function of a dimensionless "progress variable." In this case the dimensionless variable is the product of the assumed constant self-diffusion coefficient (DSD) and time (t) divided by the square of the lamellar spacing ($L = \lambda/2$). We may conclude from Figure 5 that, for example at 1200°C, no separation in β for the host and lamellae means that $[(DSD)(t)/L^2]$ is greater than 3. Thus, the "average" diffusion coefficients listed in Table 1 should be about a factor of 6 less than the Ca and Mg self-diffusion coefficients at the same temperature, if the self-diffusion coefficients are identical and independent of composition. If the self-diffusion coefficients are different and variable, as they probably are, then the "average" diffusion coefficients listed in Table 1 should approximate the minimum interdiffusion coefficient for each temperature (Brady and Yund, 1983).

The "average" diffusion coefficients of Table 1 are shown on an Arrhenius diagram in Figure 6. The arrows indicate the bracketing nature of each data point. A line drawn through the center of the brackets at 1150° and 1250°C is described by the expression

$$\tilde{D} = (3.89 \times 10^{-7}) \exp(-360.87 \text{ kJ}/RT) \quad (\text{m}^2/\text{sec}) \tag{5}$$

$$(\tilde{D} = (3.89 \times 10^{-3}) \exp(-86.25 \text{ kcal}/RT) \ (\text{cm}^2/\text{sec}))$$

although the uncertainty on the activation energy is about a factor of two. Initially, the 1100°C data do not appear to be consistent with the data for higher

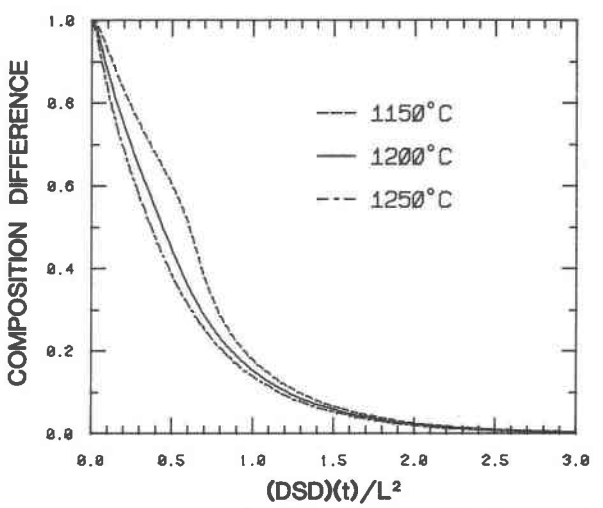

Fig. 5. The normalized differences in composition between the centers of adjacent lamellae during three numerical homogenization experiments are shown here as a function of the dimensionless time parameter $(DSD)(t)/L^2$. Differences among the curves are due entirely to the thermodynamic factor of equation (1) and Fig. 4. The finite-difference numerical experiment assumed that self-diffusion coefficients for the diffusing species (DSD) were equal and not a function of composition.

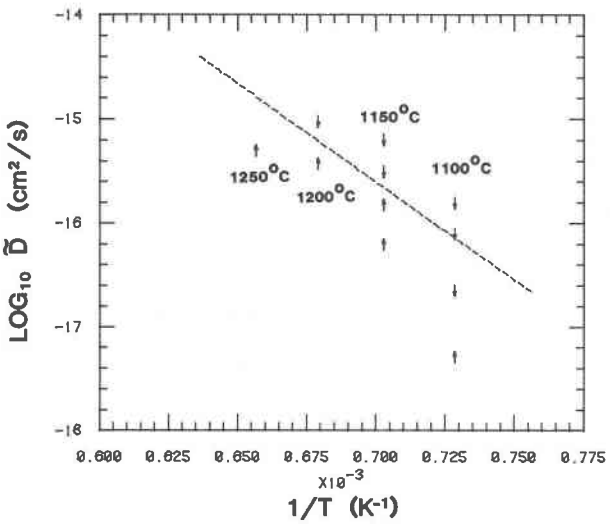

Fig. 6. The "average" diffusion coefficient brackets of Table 1 are shown here on an Arrhenius diagram. Arrows indicate the direction of each bracket. The dashed line is drawn through the midpoints of the brackets at 1150° and 1200°C and is described by equation (5). brackets at 1100°C have been disregarded for reasons described in the text.

temperatures. The 1100°C runs differ, however, in the fact that complete homogenization was not achieved. Because of the possibility that this might affect the calculated diffusion coefficients, a more elaborate numerical model was developed following the procedures of Tanzilli and Heckel (1968). This model allowed for the presence of a solvus along with the variable diffusivity discussed above. Results of the numerical experiment are shown in Figures 7a and 7b, which are analogous to Figures 3a and 3b. Evidently, the time required for completion of the partial homogenization in terms of $[(DSD)(t)/L^2]$ should be within a factor of two of the dimensionless time required for complete homogenization at other temperatures (Fig. 5). This means that the thermodynamic effect and composition gradients associated with the partial homogenization are not sufficient to explain the apparent discrepancy of the 1100°C data. However, it is clear from Figure 7a that the coherent interface must be moved in this process. We feel that the motion of the interface may significantly affect the rate of the partial homogenization so that the kinetics may not be controlled by Ca and Mg–Fe interdiffusion. The "average" diffusion coefficients for 1100°C should, therefore, be disregarded.

Ca and Fe self-diffusion

In an entirely separate set of experiments, we have attempted to obtain Ca and Fe self-diffusion data for clinopyroxenes. A "thin-film" (Shewmon, 1963, p. 7) of either ^{45}Ca or ^{57}Fe was evaporated from a chloride solution onto a polished (001) face (~2 mm square) of a diopside crystal. For the ^{45}Ca experiment a very pure diopside $Ca_{0.995}Na_{0.024}Mg_{0.989}Mn_{0.002}Fe_{0.007}Al_{0.004}Si_{1.989}O_6$ (U.S. National Museum 117733) from Natural Bridge,

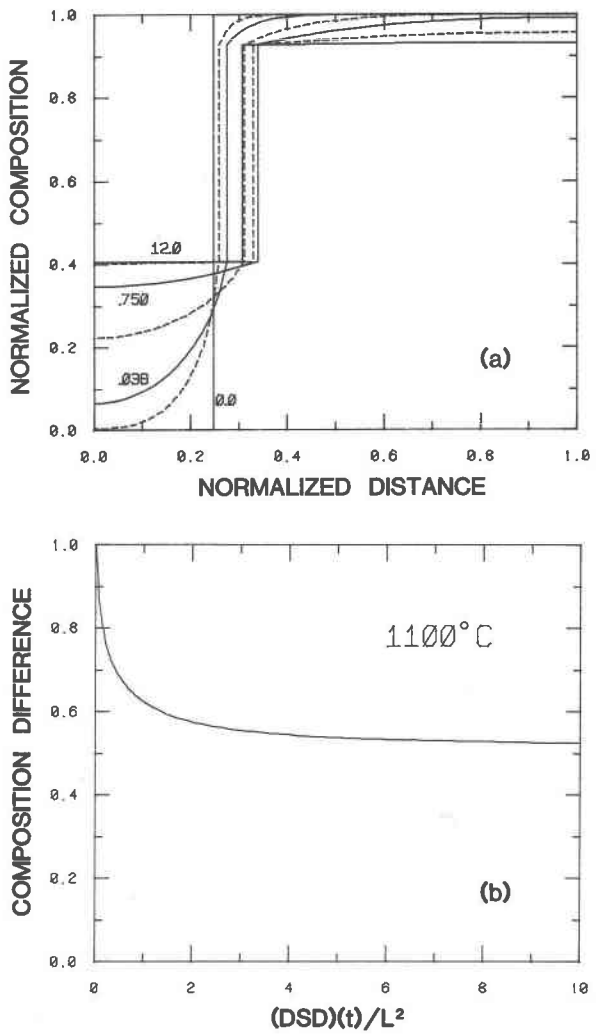

Fig. 7. (a) Normalized composition profiles for various stages in a numerical experiment simulating the partial homogenization of the Mabuki pyroxene lamellae at 1100°C and 25 kbar using procedures described by Tanzilli and Heckel (1968). Profiles are shown for values of the dimensionless time parameter $(DSD)(t)/L^2$ of 0.0, 0.0094, 0.038, 0.188, 0.750, 3.00, and 12.00. Initially, the pigeonite lamellae grow with the interface moving to the right on the figure. For $(DSD)(t)/L^2$ greater than about 0.75, however, diopside lamellae grow at the expense of pigeonite lamellae with the interface moving to the left on the figure. (b) Progress of the partial homogenization of (a) is shown in terms of the dimensionless parameter $(DSD)(t)/L^2$.

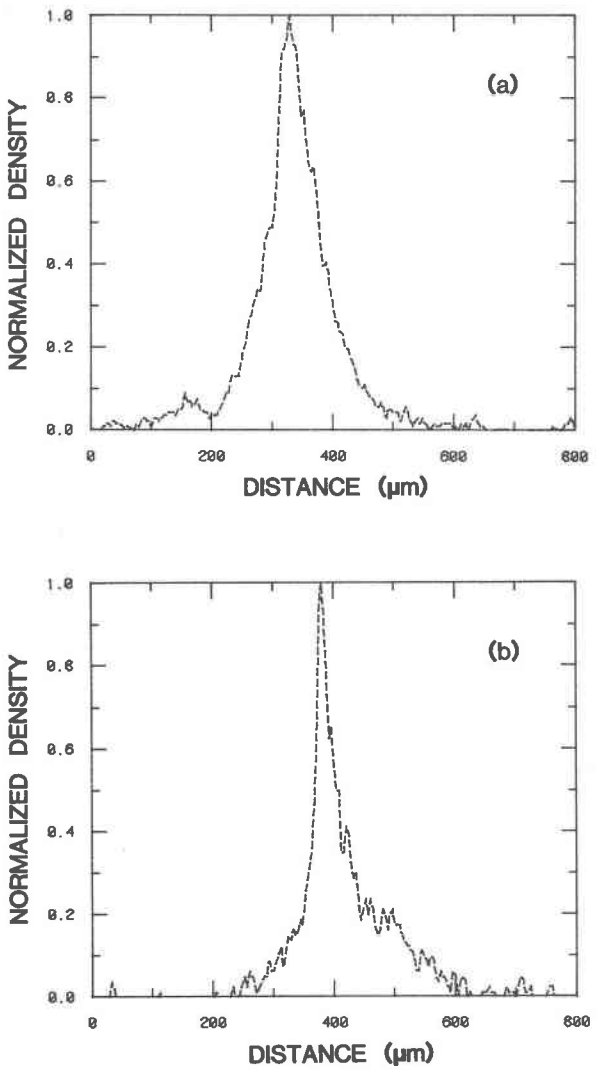

Fig. 8. "Zero time" profiles of normalized β-track density for (a) ^{45}Ca and (b) ^{57}Fe self-diffusion experiments. In each case the β-track profile is across the edge of the crystal (on the left) into the mounting epoxy (on the right). The origin of the distance axis is arbitrary because it was not possible to mark the location of the edge of the crystal on the nuclear emulsion used to record the β tracks. Neither the pyroxene nor the epoxy is "opaque" to β particles emitted by ^{45}Ca or ^{57}Fe.

NY, was used. For the ^{57}Fe experiments a diopside $Ca_{0.977}Na_{0.031}Mg_{0.953}Mn_{0.001}Fe_{0.025}Al_{0.022}Si_{1.989}O_6$ from Dekalb, New York, was used. Each crystal was pre-annealed at 830°C for 72 hours to implant the tracer, then annealed for various times from 3 weeks to 6 months at higher temperatures in air. After the experiment, the diopside crystal was mounted in epoxy, sectioned perpendicular to (001), polished flat, and exposed to a K-5 Ilford nuclear emulsion sensitive to β-particles. A β-track density profile was obtained from the developed emulsion using an optical densitometer.

Although the observed "zero-time" (pre-anneal only) β-track profiles were wider than expected (Fig. 8), clear changes in the density profiles were observed following each run (Fig. 9). Preliminary results for ^{45}Ca (McCallister *et al.*, 1979) suggested that the profiles could be interpreted in terms of diffusion. We were particularly encouraged because our results seemed to agree with the few published diffusion data available for diopside (Seitz, 1973; Sneeringer and Hart, 1978) and structurally similar wollastonite (Lindner, 1955). Subsequent experiments with very long run times (≥6 months) have

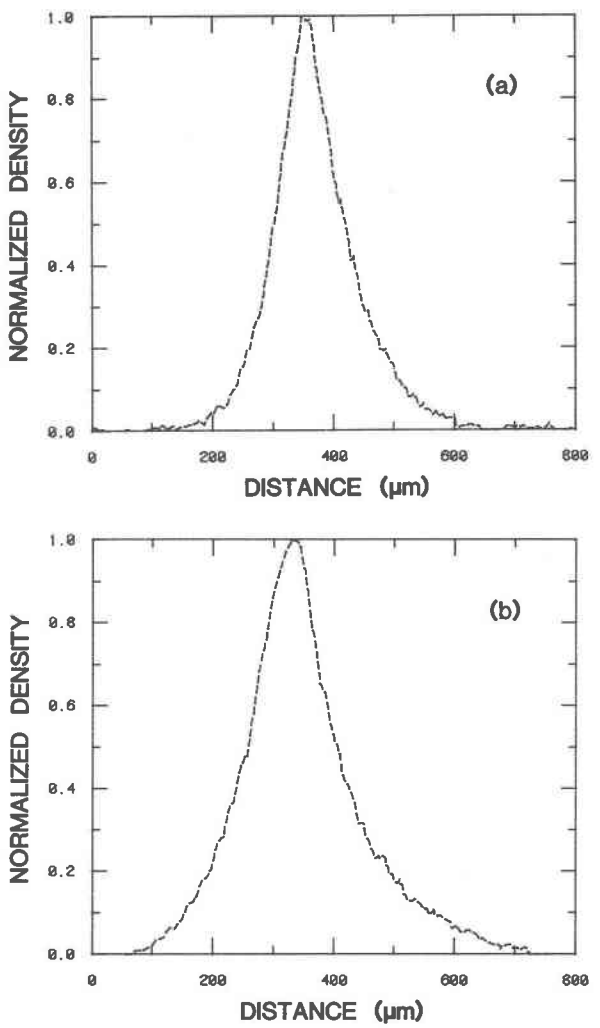

Fig. 9. Normalized β-track density profiles for self-diffusion experiments with (a) ^{45}Ca at 1300°C for 22 days and (b) ^{57}Fe at 1150°C for 207 days. In each case the crystal is on the left and the epoxy is on the right.

convinced us that the observed changes *cannot* be interpreted in terms of a simple diffusion process. Specifically, the observed profile widths do not change with time according to the expected square-root of time law. Thus, we must conclude that the self-diffusion coefficients of Ca in diopside are below our limit of detection (about 1×10^{-12} cm^2/sec at 1200°C and 2×10^{-11} cm^2/sec at 1300°C). Due to the short half-life of ^{57}Fe and the long runs required we have fewer data for Fe. Our results suggest, however, that the self-diffusion coefficient for Fe in diopside is below 2×10^{-11} cm^2/sec at 1150°C. These results are consistent with the results of our homogenization experiments.

We do not have a good explanation for the mechanism that produced the difference between Figure 8 and Figure 9. There was no evidence of recrystallization. Polished surfaces remained polished following each run. The β-track emulsions showed that the radioactive atoms did actively migrate around the surface of the crystal and into cracks if present. It is possible that a limited amount of diffusion along dislocations might have widened the profiles. However, when some of the "hot" side of the crystal was removed following one experiment, no evidence of radioactive atoms was observed at a depth of 50 microns.

Discussion

The basic point that we wish to make with this paper is that diffusion in clinopyroxenes is a comparatively slow process. Although the "average" diffusion coefficients shown in Figure 6 must be considered estimates of the minimum expected Ca–Mg interdiffusion coefficients, we believe that actual Ca–Mg interdiffusion coefficients for most Fe-poor compositions are within one or two orders of magnitude of these values. Self-diffusion coefficients for the slowest cation should be about a factor of 6 greater than the values calculated from equation (5). For physical conditions well above the clinopyroxene critical temperature (about 1500°C up to 40 kbar, Lindsley *et al.*, 1981) minimum interdiffusion coefficients could be up to about an order of magnitude higher due to a reduced thermodynamic effect.

Seitz (1973) reported Al and U tracer diffusion coefficients for diopside. His experiments involved a natural diopside annealed in a U-doped diopside–albite–anorthite melt. U diffusion coefficients were based on visual counting of β-tracks on a nuclear emulsion exposed to a cross section of his quenched experimental charge. Al profiles were measured with an electron microprobe. Seitz's results of 1×10^{-11} to 1×10^{-12} (cm^2/sec) at 1240°C are not in good agreement with our results if a simple radius and charge analogy is used. Crystal growth may have occurred in Seitz's runs. Sneeringer and Hart (1978) and Sneeringer *et al.* (1981) have reported several values for Sr tracer diffusion coefficients in natural and synthetic diopsides ranging from 1×10^{-12} to 1×10^{-16} (cm^2/sec) at 1250°C. Our data are most consistent with the lower portion of their range of values.

Freer *et al.* (1982) report the results of tracer diffusion experiments for Ca, Mg, Fe, and Al in diopside. Their "null results" (D*(Ca) and D*(Mg) $< 7 \times 10^{-14}$ cm^2/sec at 1250°C, D*(Fe) and D*(Al) $< 4 \times 10^{-14}$ cm^2/sec at 1200°C) are consistent with our data. Sanford and Huebner (1979) calculated a Ca–Mg interdiffusion coefficient for a lunar pigeonite based on the thickness of pigeonite rims on augite crystals. Their value of 4×10^{-11} (cm^2/sec) at 1050°C is well above all other reported pyroxene diffusion rates. Although the presence of iron or a high oxygen fugacity might enhance diffusion in pyroxenes as it does in olivines (Buening and Buseck, 1973; Misener, 1974), these effects would have to be quite large to reconcile our results with Sanford and Huebner's high value. Perhaps their interpretation of the development of the pigeonite rims is in error.

Although our pyroxenes had the wrong compositions to homogenize at 1 atmosphere, the work of Fernandez-Moran *et al.* (1971) and Ross *et al.* (1973) suggest that low pressure homogenization experiments can also lead to diffusion data. Fernandez-Moran *et al.* reported that a lunar pigeonite (12021,150) containing (001) augite exsolution lamellae homogenized in 8 days at 1125°C. If 60 nm is taken as the interlamellar spacing (see their Fig. 2), a lower bound to an "average" $\tilde{D}$ of 7.2×10^{-17} cm^2/sec is obtained. Miyamoto and Takeda (1977) calculated a $\tilde{D}$ from these same data but used an incorrect "infinite" diffusion model. A greater lower bound for a similar lunar (12021) pigeonite can be obtained from a homogenization experiment reported by Ross *et al.* (1973). Their crystal 3R was homogenized in 19 hours at 1176°C. Again using L = 60 nm, an "average" $\tilde{D}$ must be greater than 2.6×10^{-16} cm^2/sec. Agreement with our data is undoubtedly fortuitous, considering the differences in composition and absence of a time bracket. Huebner and Nord (1981, Fig. 6) attribute to Ross *et*

al. (1973) a much higher lower bound for $\tilde{D}$ and generally support much higher $\tilde{D}$'s for clinopyroxenes. We cannot resolve this discrepancy on the basis of the data provided in their abstract.

The validity of using homogenization experiments as described above to obtain diffusion data has been confirmed by Brady and Yund (1983) for the alkali feldspars. Interdiffusion coefficients for alkali feldspars calculated from available K and Na self-diffusion data are in good agreement with the results of cryptoperthite homogenization experiments. Price (1981) also has used homogenization experiments to obtain diffusion data for titanomagnetites, although the model used to interpret his results was slightly different from that used here. The general method has the advantages of simplicity and of access to very small diffusion coefficients. Disadvantages include the inability of the method to determine other than "average" diffusion coefficients.

Acknowledgments

This study was begun with the generous support of the Geophysical Laboratory of the Carnegie Institution of Washington. Pyroxene crystals for our experiments were supplied by R. Ryerson, B. Mason (Smithsonian), G. Harlow (American Museum), and C. Francis (Harvard). Assistance of R. Ryerson, A. Hofmann, and M. Thonnard of the Department of Terrestrial Magnetism, R. White, Smith College, and W. van Altena and J. Lee of Yale University is gratefully acknowledged. We thank M. Carpenter, R. Freer, M. Sneeringer, J. Tullis, D. Veblen, and R. Yund for careful reviews of the manuscript. This work was supported in part by NSF Grants EAR 7603804 and EAR 8001483 (McCallister). Acknowledgment is made to the Petroleum Research Fund, administered by the American Chemical Society for partial support of this research (Brady).

References

Buening, D. K. and Buseck, P. R. (1973) Fe–Mg lattice diffusion in olivine. Journal of Geophysical Research, 78, 6852–6862.

Brady, J. B. (1975) Reference frames and diffusion coefficients. American Journal of Science, 275, 954–983.

Brady, J. B. and Yund, R. A. (1983) Interdiffusion of K and Na in alkali feldspars: homogenization experiments. American Mineralogist, 68, 106–111.

Cooper, A. R., Jr. (1968) The use and limitations of the concept of an effective binary diffusion coefficient for multi-component diffusion. In J. B. Wachtman, Jr. and A. D. Franklin, Eds., Mass Transport in Oxides, p. 79–84. National Bureau of Standards Special Publication 296. U.S. Government Printing Office, Washington, D.C.

Crank, J. (1975) The Mathematics of Diffusion. Oxford University Press, London.

Darken, L. S. (1948) Diffusion, mobility, and their interrelation through free energy in binary metallic systems. American Institute of Mining and Metallurgical Engineers, Transactions, 175, 184–201.

Fernandez-Moran, H., Ohtsuki, M., and Hibino, H. (1971) Correlated electron microscopy and diffraction of lunar clinopyroxenes from Apollo 12 samples. Proceedings of the Second Lunar Science Conference, 1, 109–116.

Freer, R., Carpenter, M. A., Long, J. V. P., and Reed, S. J. B. (1982) "Null result" diffusion experiments with diopside: implications for pyroxene equilibria. Earth and Planetary Science Letters, 58, 285–292.

Huebner, J. S. and Nord, G. L., Jr. (1981) Assessment of diffusion in pyroxenes: what we do and do not know. Lunar and Planetary Science XII, 479–481. Lunar Science Institute, Houston.

Huebner, J. S., Ross, M., and Hicking, N. (1975) Significance of exsolved pyroxenes from lunar breccia 77215. Proceedings of the 6th Lunar Science Conference, 529–546.

Lindner, R. (1955) Studies on solid state reactions with radiotracers. Journal of Chemical Physics, 23, 410–411.

Lindsley, D. H., Grover, J. E., and Davidson, P. M. (1981) The thermodynamics of the $Mg_2Si_2O_6$–$CaMgSi_2O_6$ join: a review and an improved model. In R. C. Newton, A. Navrotsy and B. J. Wood, Eds., Thermodynamics of Minerals and Melts, p. 149–175. Springer-Verlag, New York.

Manning, J. R. (1968) Diffusion Kinetics for Atoms in Crystals. Van Nostrand, Princeton.

McCallister, R. H. (1977) Coherent exsolution in Fe-free pyroxenes. American Mineralogist, 62, 721–726.

McCallister, R. H. and Brady, J. B. (1979) Self-diffusion of calcium in diopside (abstr.). Geological Society of America Abstracts with Programs, 11, 474.

McCallister, R. H., Brady, J. B., and Mysen, B. O. (1979) Self-diffusion of calcium in diopside. Carnegie Institution of Washington Yearbook, 78, 574–577.

Miyamoto, M. and Takeda, H. (1977) Evaluation of a crust model of eucrites from the width of exsolved pyroxene. Geochemical Journal, 11, 161–169.

Misener, D. J. (1974) Cationic diffusion in olivine to 1400°C and 35 kbar. In A. W. Hofmann, B. J. Giletti, H. S. Yoder, Jr., and R. A. Yund, Eds., Geochemical Transport and Kinetics, p. 117–129. Carnegie Institution of Washington, Washington, D.C.

Nixon, P. H. and Boyd, F. R. (1973) Petrogenesis of the granular and sheared ultrabasic nodular suite in kimberlites. In P. H. Nixon, Ed., Lesotho Kimberlites, p. 48–56. Lesotho National Development Corporations, Maseru.

Price, G. D. (1981) Diffusion in the titanomagnetite solid solution series. Mineralogical Magazine, 44, 195–200.

Reynolds, J. E., Averbach, B. L., and Cohen, M. (1957) Self-diffusion and interdiffusion in gold-nickel alloys. Acta Metallurgica, 5, 29–40.

Ross, M., Huebner, J. S., and Dowty, E. (1973) Delineation of the one-atmosphere augite–pigeonite miscibility gap for pyroxenes from lunar basalt 12021. American Mineralogist, 58, 619–635.

Sanford, R. F. and Huebner, J. S. (1980) Re-examination of diffusion processes in 77115 and 77215. Lunar Science X, 1052–1054. Lunar Science Institute, Houston.

Seitz, M. G. (1973) Uranium and thorium diffusion in diopside and fluorapatite. Carnegie Institution of Washington Yearbook, 72, 586–588.

Shewmon, P. G. (1963) Diffusion in Solids. McGraw Hill, New York.

Sneeringer, M. and Hart, S. (1978) Sr diffusion in diopside

(abstr.). EOS, American Geophysical Union Transactions, 59, 402.

Sneeringer, M., Hart, S., and Shimizu, N. (1981) Diffusion of strontium in diopside: a comparison of ion microprobe and radiotracer analytical methods (abstr.). EOS, American Geophysical Union Transactions, 62, 428–429.

Tanzilli, R. A. and Heckel, R. W. (1968) Numerical solutions to the finite, diffusion-controlled, two-phase, moving-interface problem (with planar, cylindrical, and spherical interfaces). Transactions of the Metallurgical Society of AIME, 242, 2313–2321.

Thompson, J. B., Jr. and Waldbaum, D. R. (1969a) Analysis of the two-phase region halite–sylvite in the system NaCl-KCl. Geochimica et Cosmochimica Acta, 33, 671–690.

Thompson, J. B., Jr. and Waldbaum, D. R. (1969b) Mixing properties of sanidine crystalline solutions: III. Calculations based on two-phase data. American Mineralogist, 54, 811–838.

Tullis, J. and Yund, R. A. (1979) Calculation of coherent solvi for alkali feldspar, iron-free clinopyroxene, nepheline–kalsilite, and hematite–ilmenite. American Mineralogist, 64, 1063–1074.

Turnock, A. C., Lindsley, D. H., and Grover, J. E. (1973) Synthesis and unit cell parameters of Ca–Mg–Fe pyroxenes. American Mineralogist, 58, 50–59.

Manuscript received, January 22, 1982;
accepted for publication, August 17, 1982.